

A search for period changes of eight short-period Type II Cepheids

Alemiye M. Yacob,^{1,2,3*}† Leonid N. Berdnikov,⁴ Elena N. Pastukhova,⁵ Alexei Y. Kniazev,^{3,4,6}
Patricia A. Whitelock^{3,7}

¹ Astronomy and Astrophysics Department, Entoto Observatory and Research Center (EORC), Space Science and Geospatial Institute (SSGI), P.O. Box 33679, Addis Ababa, Ethiopia

² Addis Ababa University (AAU), P.O.Box 1176, Addis Ababa, Ethiopia

³ South African Astronomical Observatory (SAAO), P.O. Box 9, 7935 Observatory, Cape Town, South Africa

⁴ Sternberg Astronomical Institute (SAI) of the Moscow State University, Universitetskii pr. 13, 119992 Moscow, Russia

⁵ Institute of Astronomy, Russian Academy of Sciences, Pyatnitskayaul. 48, 119017 Moscow, Russia

⁶Southern African Large Telescope (SALT) Foundation, P.O. Box 9, 7935 Observatory, Cape Town, South Africa

⁷ Department of Astronomy, University of Cape Town, 7701 Rondebosch, South Africa

Accepted 2022 July 28. Received 2022 July 28; in original form 2022 June 28

ABSTRACT

In this study, we investigate the period changes of eight short-period Type II Cepheids of the BL Her subtype, i.e., with periods in the 1–4 day range. The $O - C$ diagrams for these stars are constructed using all suitable observational data from ground and space surveys. This spans a time interval of over one century and includes digitized photographic plates as well as photometry from the literature. The $O - C$ diagrams show parabolic evolutionary trends, which indicate the presence of both increasing and decreasing periods for these eight short period stars. These period changes are in good agreement with the recent theoretical evolutionary framework and stellar evolution models for BL Her stars. The pulsation stability test proposed by Lombard and Koen also suggests that the changes in the periods are real.

Key words: stars: variables: Cepheids – stars: Population II – stars: evolution – stars: low-mass– methods: data analysis

1 INTRODUCTION

Type II Cepheids (T2Cs) are old, low-mass and radially pulsating variable stars with luminosities below the classical Cepheids and above the RR Lyraes (RRLs) in the Hertzsprung-Russell diagram (e.g., [Wallerstein 2002](#)).

T2Cs are in the post-horizontal branch evolutionary phase of low-mass stars, where double shell (hydrogen and helium) burning occurs in thin shells outside the inert carbon-oxygen core. As it ascends the asymptotic giant branch (AGB) the star expands rapidly and becomes cooler and brighter. It experiences shell flashes at the boundary between the core and the helium shell. During these shell flashes the radius decreases temporarily; thus, the star moves to higher temperatures and into the instability strip (IS). As these stars leave the horizontal branch (HB) and evolve further up the AGB, they cross the IS at higher luminosity than RRLs and become T2Cs (see, e.g., [Bhardwaj 2022](#); [Catelan & Smith 2015](#), and reference therein).

Based on their pulsation periods T2Cs are classified as BL Herculis (BLHs) for periods between 1 and 4 days, W Virginis (WVs) for periods greater than four and less than 20 days, and RV Tauri (RVs) stars for period greater than 20 days (e.g., [Soszyński et al. 2018](#)).

The three grouping of T2Cs represent various stages of post-

horizontal branch evolution. In each evolutionary stage, predicted stellar properties can be compared with observations. Short-period T2Cs stars crossing the IS show increasing periods as they evolve redward from the HB to the AGB. The intermediate-period WVs, evolving at higher luminosities on the AGB, suffer helium shell flashes and are making temporary excursions from the AGB into the IS, showing either increasing or decreasing periods. RVs stars, with long periods, are post-AGB stars undergoing thermal pulses that send them blueward into the IS and show only decreasing periods ([Gingold 1976](#); [Bono et al. 1997b](#); [Wallerstein 2002](#)).

The period change is one of the essential properties of pulsating stars obtained directly from observational data that can be used to constrain and test stellar structure models and to probe stellar evolution. The period change is thus one of the parameters that can detect evolutionary effects on human time-scales.

Several studies have been conducted to investigate the pulsation and evolutionary status of T2Cs as described in reviews by [Wallerstein \(2002\)](#) and [Neilson et al. \(2016\)](#). A number of theoretical evolutionary track grids and pulsation models have been developed (see e.g., [Gingold 1976](#); [Bono et al. 1997a,b, 2016, 2020](#); [Smolec 2016](#); [Dotter 2008](#); [Dell’Omodarme et al. 2012](#)) that can be used to compute the pulsation properties including period changes, period distributions, crossing modes and other characteristics of T2Cs in their post-HB evolution.

From theoretical considerations we would expect short-period T2Cs (BLH) stars, to be dominated by increasing periods as the they move redward from the hot edge to the cool edge of the IS (e.g.,

* E-mail: alemiyem@essti.gov.et (AMY)

† Research visitor @ SAAO, SA

Gingold 1976; Bono et al. 2016; Sandage et al. 1994; Wallerstein 2002).

Several period change studies of BLH stars in globular clusters (Osborn 1969; Wehlau & Bohlender 1982; Juresik et al. 2001; Osborn et al. 2019) and in the field (Christianson 1983; Diethelm 1996; Provencal 1986) have found that the majority of BLH stars do indeed show period increases while a minority, within observational uncertainties and limited data, show no period change. However, the changes are broadly consistent with theoretically predicted period changes (Neilson et al. 2016; Smith 2013).

For BLH stars, the most apparent evolutionary trend is redward evolution with an increasing period. However, Gonzales (1994) discovered one example that demonstrated blue-ward advancement with a decreasing period. Furthermore, the current theoretical framework (Bono et al. 2020) predicts that BLH stars can experience both negative and positive period changes during their post-HB evolution. This prediction was based on gravo-nuclear instabilities at the onset of He-shell burning, following the exhaustion of helium in the core. The existence of these ‘gravo-nuclear loops’(GNLs) causes BLH stars to stay longer inside the IS and make fast period changes (Bono et al. 1997a,b). Such scenarios would suggest that BLHs could show alternately increasing and decreasing periods on quite short timescales. The period changes found in our study of BLH stars support the existence of GNLs, and if interpreted in terms of breathing pulses they could provide new insight into the very uncertain mixing processes which are crucial for stellar evolution (see also Sweigart et al. 2000).

In this work, we revise and study the period changes of eight BLH stars, with periods between 1 and 2 days, which are usually called *Above Horizontal Branch* (AHB) stars (Diethelm 1983) during their post-HB evolution. We also investigate the evolutionary changes in period of BLHs from records dating back over a century and compare them to those predicted by the theory of stellar evolution. The eight BLH stars, in order of increasing period, are V716 Oph, BF Ser, CE Her, BL Her, XX Vir, KZ Cen, V745 Oph, and V439 Oph; they are listed in Table 1.

This paper is structured as follows: in section 2 we describe the data sources, methods and analyses used for this study. In section 3 we present and discuss the result of our work by comparing it with theoretical models and previous observational analyses. Finally, section 4 provides a summary and conclusion.

2 DATA, METHODS AND ANALYSIS

For this research, we used all suitable (B , V , and g') band data we could find in the literature, from ground- and space-based surveys, including digitized photographic plates. Specifically, we used: (i) photographic (PG) data from Digital Access to a Sky Century at Harvard (DASCH) (Grindlay et al. 2012), and from the Sternberg Astronomical Institute (SAI); (ii) CCD data (filters V and g') from the All Sky Automated Surveys (ASAS-3) (Pojmanski 2002), the All Sky Automated Surveys of SuperNovae (ASAS-SN) (Kochanek et al. 2017), INTEGRAL-OMC (Alfonso-Garzón et al. 2012), Catalina Sky Survey (CSS) (Drake et al. 2013), PAN-STARSS (Chambers et al. 2016), HIPPARCOS (Perryman et al. 1997); (iii) photoelectric (PHE) (filters B and V), visual (VIS) and photovisual (PGV) data from the literature. The photographic data, from DASCH, SAI and others, obtained from the literature are assumed to be identical to B -band photometry for the purpose of this analysis.

We present the general information for the stars from the general catalogue of variable stars (GCVS) (Samus' et al. 2017) in Table 1. All other data sources used for this study are listed in Table 2.

Table 1. Summary of information for the BLH stars from the GCVS.

Star	Period [d]	Max V [mag]	Min V [mag]
V716 Oph	1.116	11.28	12.60
BF Ser	1.165	11.05	12.56
CE Her	1.209	11.53	12.92
BL Her	1.307	9.70	10.62
XX Vir	1.348	11.55	12.78
KZ Cen	1.520	11.80	12.77
V745 Oph	1.595	12.70	13.90
V439 Oph	1.893	11.73	12.70

The data obtained from different sources are combined and sorted in order of Heliocentric Julian Date (HJD). They are then divided into seasonal batches, generally covering intervals of at least 3-months each year, although this obviously depends on the individual data sets and the length of the gaps between them. For the PG data there are sometimes gaps of several years between data-sets. The seasonal light-curves generated for each data-batch were then used to construct the $O - C$ curves.

To search for any period changes we employed the observed minus calculated ($O - C$) time of maximum as illustrated in an $O - C$ diagram. The observed light-curves (O) were constructed for each star at each season and then compared with a reference light-curve (C) to calculate the difference between the times of maximum light ($O - C$). The $O - C$ residuals were determined using the Hertzsprung (1919) method, with the algorithm developed by Berdnikov (1992). At the same time we correct for the shifts in the time of maxima between observations made through different filters. We use the method by Lombard & Koen (1993) to confirm that the pulsation period changes are real.

Assuming that the change in a period is linear with time, we can calculate the maximum light elements for all stars using the following quadratic elements (Sterken 2005) :

$$HJD_{\max} = M_0 + PE + QE^2, \quad (1)$$

where P is the period at the adopted epoch, M_0 , Q is a parabolic term and E is the number of the cycle. The quadratic coefficient Q relates to $O - C$ with the following equation :

$$Q = \frac{1}{2} \frac{dp}{dt} P_{\text{mid}} E^2, \quad (2)$$

where dP/dt is the rate of period change and P_{mid} is the mid-epoch period.

The quadratic coefficient Q can be used to measure the values of period change (dP/dt) in seconds per year (s/yr) or in days per million years (d/Myr) using the following relations in Eqn. 3 and 4, respectively, using sidereal years:

$$\frac{dP}{dt} = 365.25 \times 24 \times 60 \times 60 \times \left(\frac{2Q}{P_{\text{mid}}} \right), \quad (3)$$

$$\frac{dP}{dt} = 730.5 \times 10^6 \times \left(\frac{Q}{P_{\text{mid}}} \right). \quad (4)$$

Table 2. Summary of the Data Sources

Star Name	JD & Year Intervals	No. of Observ.	Type of Observation	References
V716 Oph	2411544 - 2458589 1890 - 2019	2041	PG	DASCH
		199	PG	Mandel (1970) ; Kinman et al. (1984) ; Kinman (1965)
		117	PG	SAI
		17	CCD (g')	PAN-STARSS
		126	CCD (V)	INTEGRAL- OMC
		176	PHE (B,V)	Kwee & Diethelm (1984) ; Diethelm (1986) ; Lin (1983) McNamara & Pyne (1994) ; Bookmeyer et al. (1977)
		330	CCD (V)	CSS
		1448	CCD (g',V)	ASAS-SN
		509	CCD (V)	ASAS3 2411549
		2226	PG	DASCH
BF Ser	2411549 - 2458589 1890 - 2019	780	PG VIS	Ashbrook (1950) ; Soloviev (1952) ; Mandel (1970) ; Nikulina (1966)
		69	PG	SAI
		11	CCD (g')	PAN-STARSS
		132	CCD (V)	INTEGRAL-OMC
		126	CCD (V)	HIPPARCOS
		128	PHE (B,V)	Henden (1996) ; Diethelm & Tamman (1982) ; Harris (1980) Ashbrook (1950); Soloviev (1952); Bookmeyer et al. (1977)
		367	CCD (V)	CSS
		1510	CCD (g',V)	ASAS-SN
		355	CCD (V)	ASAS3
		1584	PG	DASCH
CE Her	2411586 - 2458589 1890 - 2019	247	PG	VIS
		9	CCD (g')	PAN-STARSS
		118	CCD (V)	INTEGRAL-OMC
		189	PHE (B,V)	Loomis et al. (1988) ; Chambers et al. (2016) Harris(1980); Diethelm & Tamman (1982)
		101	CCD (V)	CSS
		1591	CCD (g',V)	ASAS-SN
		4449	PG	DASCH
		504	PG & PGV	Mandel(1970)
		54	CCD (V)	INTEGRAL-OMC
		123	CCD (V)	HIPPARCOS
Bl Her	2411508 - 2458589 1890 - 2019	658	PHE (B,V)	Mitchell et al. (1964) ; Moffett & Barnes (1984) Arellano Ferro et al. (1998); Alexander et al. (1987); Meakes et al. (1991) Michałowska-Smak & Smak (1965); Preston & Kilstorn (1967) Ignatova & Vozyakova (2000); Szabados (1977); Harris(1980)
		1647	CCD (g',V)	ASAS-SN
		495	CCD (V)	ASAS3
		1832	PG	DASCH
		639	PG & VIS	Oosterhoff (1936) ; Mandel (1970)
		13	CCD (g')	PAN-STARSS
		68	CCD (V)	INTEGRAL-OMC
		214	PHE (B,V)	Bookmeyer et al. (1977), Loomis et al. (1988) Harris (1980); Mitchell et al. (1964); McNamara & Pyne (1994)
		302	CCD (V)	CSS
		1548	CCD (g',V)	ASAS-SN
KZ Cen	2411167 - 2458590 1889 - 2019	1527	PG	DASCH
		190	PHE (B,V)	Petersen & Hansen (1984) ; Irwin (1961) ; Diethelm (1986)
		1907	CCD (g',V)	ASAS-SN
		617	CCD(V)	ASAS3
V439 Oph	2410929 - 2458589 1888 - 2019	1626	PG	DASCH
		236	PGV & VIS	Mandel (1970); Tsesevich (1952)
		258	PG	SAI
		10	CCD (g')	PAN-STARSS
		26	CCD (V)	INTEGRAL-OMC
		61	PHE (B,V)	Sturch (1966) ; Henden (1980) ; Diethelm & Tamman (1982) ; Diethelm (1986)
		1019	CCD(g',V)	ASAS-SN
		177	CCD(V)	ASAS3
		1217	PG	DASCH
		193	PGV & VIS	Mandel(1970)
V745 Oph	2412263 -2458589 1892 - 2019	12	CCD(g')	PAN-STARSS
		80	CCD (V)	INTEGRAL-OMC
		41	PHE (B,V)	Kwee & Diethelm (1984) ; Diethelm (1986)
		114	CCD (V)	CSS
		1567	CCD (g',V)	ASAS-SN

3 RESULTS AND DISCUSSION

We have calculated for the eight BLHs: the quadratic elements, the rates of period change and the corrections for maxima in the B - and g' -bands, as listed in Tables 3 and 4. We constructed the $O - C$ diagrams for each star with all available data and performed the corresponding period change test to confirm whether the period changes are real or not. The resulting $O - C$ diagrams and the period change test graphs are presented in Figures 1 and 2, respectively.

In the $O - C$ diagrams, we see convex parabolas (e.g., BL Her in Fig. 1) indicating increasing periods and concave parabolas (e.g., V745 Oph in Fig. 1) indicating decreasing periods. Thus we have examples of both increasing and decreasing periods within this sample of eight stars.

The results from the seasonal light-curves for all our objects are presented in the appendix (supplementary materials) Table A1. Columns 1, 2 and 3 give the times of maximum light and their errors; column 4 gives the type of observations used; columns 5 and 6 contain the epoch number E and the $O - C$ residual; columns 7 and 8 contain the number of observations N and the data sources, respectively. The data from Table A1 are shown on the $O - C$ diagrams (Fig. 1) as open squares for the Harvard photographic measurements and as dots for all the remaining observations, with vertical bars indicating the limits of the errors in the $O - C$ residuals. The parabolic elements obtained for the stars are listed in Table 3.

It is well known that the brightness maxima for pulsating variables generally occur later at longer wavelengths. This differences in the light curves from different filters was first noted by Arp (1955), who demonstrated that the times of maximum and minimum in the V -band (M_V) light-curves lag behind those in the B -band (M_{PG}) light-curves. When different passbands are simultaneously present in the observational data set, the primary passband should be selected in order to determine the shifts in the times of maximum light in other bands. In our case, among the three bands used (V , B , and g'), the V -band is our primary reference. Accordingly, we make the phase shift in the times of maximum for the B - and g' -bands with respect to the V -bands, which is reported in days. The phase shifts are expressed as $\Delta\phi(B,V) = \phi_B - \phi_V$ and $\Delta\phi(g',V) = \phi_{g'} - \phi_V$. These corrections for maxima in the B - and g' -bands are given in Table 4. We applied them when constructing Fig. 1 and determining the elements (Table 4) which refer to the V -band. The quadratic elements (Table 3) make it possible to calculate the rate of change in the period (dP/dt), which is given in column 5 of Table 4, together with its error.

Assuming a constant rate of change for the periods We applied parabolic fits to the $O - C$ diagrams. We do see irregular changes, that do not fit the parabolic pattern, in some of the diagrams (V716 Oph, BF Ser, BL Her, Ce Her & XX Vir); these changes could be the result of random fluctuation in the periods. Such random fluctuations have been observed in classical Cepheid variables. The Eddington & Plakidis (1929) method can be used to test for random, cycle-to-cycle changes in period, and it is usually applied to long-period Cepheids. For short period Cepheids, the Lombard & Koen (1993) method is useful to check whether the period change is real or due to random fluctuations.

For the BLHs we used the Lombard & Koen method for every star to check whether the measured $O - C$ residuals indicate real period changes. For this purpose, we calculated the differences $\Delta(O - C)_i$ of successive $O - C$ residuals from Table A1, $\Delta(O - C)_i = (O - C)_{i+1} - (O - C)_i$, and plotted $D_i = \Delta(O - C)_i/(E_{i+1} - E_i)$ against $E'_i = (E_i + E_{i+1})/2$ (Fig. 2). The differences, D_i , which describe the period changes in the epoch interval $E_i - E_{i+1}$, correspond to the behaviour of the O-C residuals in Fig. 1. As shown in Fig. 2, the

Table 3. The quadratic elements

Stars	$HJD_{max} = M_o + PE + QE^2$, where M_o adopted epoch, P is the period at adopted epoch and Q is parabolic term
V716 Oph	$2435904.8889 + 1.1159169E + 0.34152 \times 10^{-10}E^2$
BF Ser	$2437226.1635 + 1.1654399E - 0.55228 \times 10^{-10}E^2$
CE Her	$2436639.7693 + 1.2094373E + 0.15322 \times 10^{-9}E^2$
BL Her	$2436482.0464 + 1.3074548E - 0.68189 \times 10^{-9}E^2$
XX Vir	$2436163.5888 + 1.3482049E - 0.68355 \times 10^{-10}E^2$
KZ Cen	$2435356.4024 + 1.5199792E + 0.24842 \times 10^{-8}E^2$
V745 Oph	$2435965.8617 + 1.5951035E + 0.52379 \times 10^{-7}E^2$
V439 Oph	$2435842.2304 + 1.8929943E + 0.19312 \times 10^{-8}E^2$

differences D_i in pulsation period show decreases and increases as a function of time.

From our period derivative results, we found a decreasing period for three stars, namely BF Ser, BL Her, and XX Vir, and an increasing period for the remaining five stars, namely V716 Oph, CE Her, KZ Cen, V745 Oph, and V439 Oph. The period-change graph for V716 Oph, illustrated in Fig. 2, is almost flat, making it difficult to see if there is any significant change at all. Nevertheless, our analysis indicated an increasing period of 0.022 ± 0.0048 d/Myr. In a prior study by Diethelm (1996), XX Vir and BF Ser showed no period changes and constant period change, respectively, over 70 years. However, in the current study, we found decreasing periods over the 129-year span. For V716 Oph and CE Her our result and Diethelm's show increasing periods, although there are slightly different period changes. For the remaining stars, we found positive (KZ Cen, V439 Oph, & V745 Oph) and negative (BL Her) period changes. The measured rate of period change in all eight BLH stars is in the range 10^{-5} and 10^{-8} days per year, which is the same order of magnitude as estimated by Sandage et al. (1994), Wehlau & Bohlender (1982), Diethelm (1996) and Osborn et al. (2019) for stars evolving from the HB towards the AGB. In addition, the parabolic trends of the $O - C$ diagrams suggests that the observed rate of period change can be understood as real evolutionary changes.

3.1 Comparison with theoretical prediction of period change by Bono et al. 2020

Several studies have been conducted to examine the evolutionary status of post-horizontal branch stars by constructing models and deriving evolutionary tracks for stars leaving the HB (e.g. Gingold 1976; Bono et al. 1997a,b; Dotter 2008; Dell'Ombrone et al. 2012). The evolutionary models of blue HB stars with depleted core helium show three different evolutionary paths depending on their mass on the HB (Bono et al. 2016). The first path is for low mass stars ($M/M_\odot \lesssim 0.515$), these do not enter the IS and never reach the AGB. They move into their white dwarf cooling sequence and are usually referred to as AGB-Manqu  stars. The second path is for more massive stars ($0.52 \lesssim M/M_\odot \lesssim 0.62$), these evolve redward through the IS, above the HB as they move towards their AGBs. They are known as Post-Early AGB (PEAGB). The third path is for higher mass stars ($0.62 \lesssim M/M_\odot \lesssim 0.80$), which evolve along the AGB and into the Post-AGB phase (PAGB). They also experience thermal pulses and are therefore known as thermally pulsating AGB (TPAGB) stars. The BLH stars are thus classified as PEAGB stars that evolve redward en route to the AGB by crossing the IS (Bono et al. 2020).

Table 4. Corrections for maxima in the B - and g' -bands and rate of period change.

Stars	Difference between V - & B -bands $\Delta\phi(B, V)$ [d]	Difference between V - & g' -bands $\Delta\phi(g', V)$ [d]	New Element	Rate of Period change (s/year)
V716 Oph	0.0006	0.0048	2435904.8889 + 1.1159169 E	0.00193 ± 0.00042
BF Ser	-0.0037	0.0067	2437226.1635 + 1.1654399 E	-0.00299 ± 0.00031
CE Her	-0.0044	-0.0020	2436639.7693 + 1.2094373 E	0.008 ± 0.00068
BL Her	0.00070	-0.0069	2436482.0464 + 1.3074548 E	-0.03292 ± 0.00050
XX Vir	0.00999	0.00608	2436163.5888 + 1.3482049 E	-0.0032 ± 0.00029
KZ Cen	-0.0016	-0.0018	2435356.4024 + 1.5199792 E	0.10315 ± 0.00119
V745 Oph	-0.0147	-0.0135	2435965.8617 + 1.5951035 E	2.07251 ± 0.00770
V439 Oph	0.0050	0.0249	2435842.2304 + 1.8929943 E	0.06439 ± 0.00346

According to the evolutionary analysis of T2Cs by Gingold (1976, 1985), BLHs on their way to the AGB experience blue-loops, known as ‘blue-noses’, after crossing the IS. Before the BLHs reach the AGB the ‘blue-nose’ causes two additional crossings of the IS. Gingold argues that the reason for these three successive excursions is a readjusting of the hydrogen and helium-burning shells before the stars reached the AGB. However, recent evolutionary studies and HB evolutionary models with updated physics inputs do not support the scenario proposed by Gingold (Bono et al. 2016).

Bono et al. (1997a,b) proposed a model that involves several GNLs in the Hertzsprung-Russell diagram that the BLH star encounters before it reaches the AGB. They pointed out that the ignition of the helium-shell in PEAGB BLH stars is dramatically different from the normal evolutionary process. Following core helium exhaustion helium-shell burning started immediately, causing the structure to expand rapidly and creating a large discontinuity of energy sources in both the hydrogen and helium shells, that resulted in GNLs. The helium-burning shell undergoes a series of gravo-nuclear instabilities before the star resumes its normal evolutionary path to the AGB.

Sweigart et al. (2000) investigated the GNLs reported by Bono et al. (1997a,b) during the onset of helium-shell burning at the end of the HB phase. They discovered the occurrence of GNLs, characterized by relaxation oscillations within the helium shell, that led to loops in the evolutionary tracks. Sweigart et al. showed that the onset of helium-burning produces GNLs in the shell immediately following core-helium exhaustion, and indicated their strong dependence on the helium profile. They also argued that the treatment of convective boundaries following core helium burning (CHeB) impacts on the presence of GNLs. Constantino et al. (2016) further demonstrating that at the end of CHeB, the helium-shell encountered convective overshooting at the convective boundary, whereby the GNLs appeared during the early AGB phase. Both the Sweigart et al. and Constantino et al. studies supported the existence and effects of GNLs during early AGB evolution.

Bono et al. (2020) recently presented a theoretical framework that examines the evolutionary and pulsation properties of T2Cs based on HB evolutionary models. They predicted that BLH stars would show both positive and negative period changes. The prediction assumes the occurrence of multiple GNLs at the onset of He-shell burning. Such loops could also result in increased time spent within the IS and rapid period changes for the BLH stars in this short period regime.

In our study, we found both positive and negative period changes for BLH stars during their PEAGB phases in agreement with the Bono et al. (2020) predictions.

The detection of period changes that agree with the current theoretical framework proposed by Bono et al. (2020) has significance

in modelling the GNLs, and many also contribute to providing detailed information about the occurrence of breathing pulses relevant to understanding Helium-burning mixing process that are important to our understanding of stellar evolution.

3.2 Comparison with predicted period change of evolutionary track model and results of Osborn et al. 2019

3.2.1 Comparison with predicted period changes and crossing modes

Osborn et al. (2019) conducted a period change analysis for metal-poor BLH stars identified in the M13 globular cluster. They calculated the observed rate of period change for three BLH stars using $O - C$ method, and found increasing periods for all of them.

To compare the results of the measured period changes with evolution models Osborn et al. constructed colour-magnitude diagrams for M13 showing BLH and RRL stars overlaid with post-horizontal branch tracks from the models of the Pisa group (Dell’Omodarme et al. 2012). To understand the evolutionary stages and determine the pulsation period change rate, the Pisa evolutionary tracks are divided into three phases related to the ‘blue loop’. These are: pre-loop, the first redward evolution (FRE) for the crossing of the IS, where the star’s period is expected to increase; blueward evolution (BE), where the period decreases; and post-loop as the second redward evolution (SRE), where the period increases as the star resumes its evolution towards the AGB.

Osborn et al. estimated the rates of period change (dP/dt) using the Pisa models and presented a graph of dP/dt versus P (their fig. 9). From this diagram, all M13 stars are found to be located in the SRE phases, and the measured period changes of BLH stars are in qualitative agreement with theoretical predictions of post-HB evolution. Osborn et al. argued that this $dP/dt - P$ diagram, with Pisa evolutionary tracks, can be extended and used for other BLH stars to estimate their evolutionary stage and directions while crossing the IS. Accordingly, Osborn et al. determined the crossings made for 18 BLH stars with published period changes, on the $dP/dt - P$ diagram.

Based on the Osborn et al. work, we compared our results with the Pisa models, using evolutionary tracks with $Y = 0.25$, and indicate the crossing mode of our stars (red diamonds) in the $dP/dt - P$ diagram as shown in Fig. 3 (Osborn et al. 2019, private communication 2022).

From Fig. 3, we are able to locate our stars in the FRE, BE and SRE stages, along with the other 18 BLH stars. The crossing modes for each evolutionary stage are presented in Table 5; one star is in the FRE, four in the SRE and three in the BE stages. For comparison and future use we include published period change rates for BLHs with our result in Table 6.

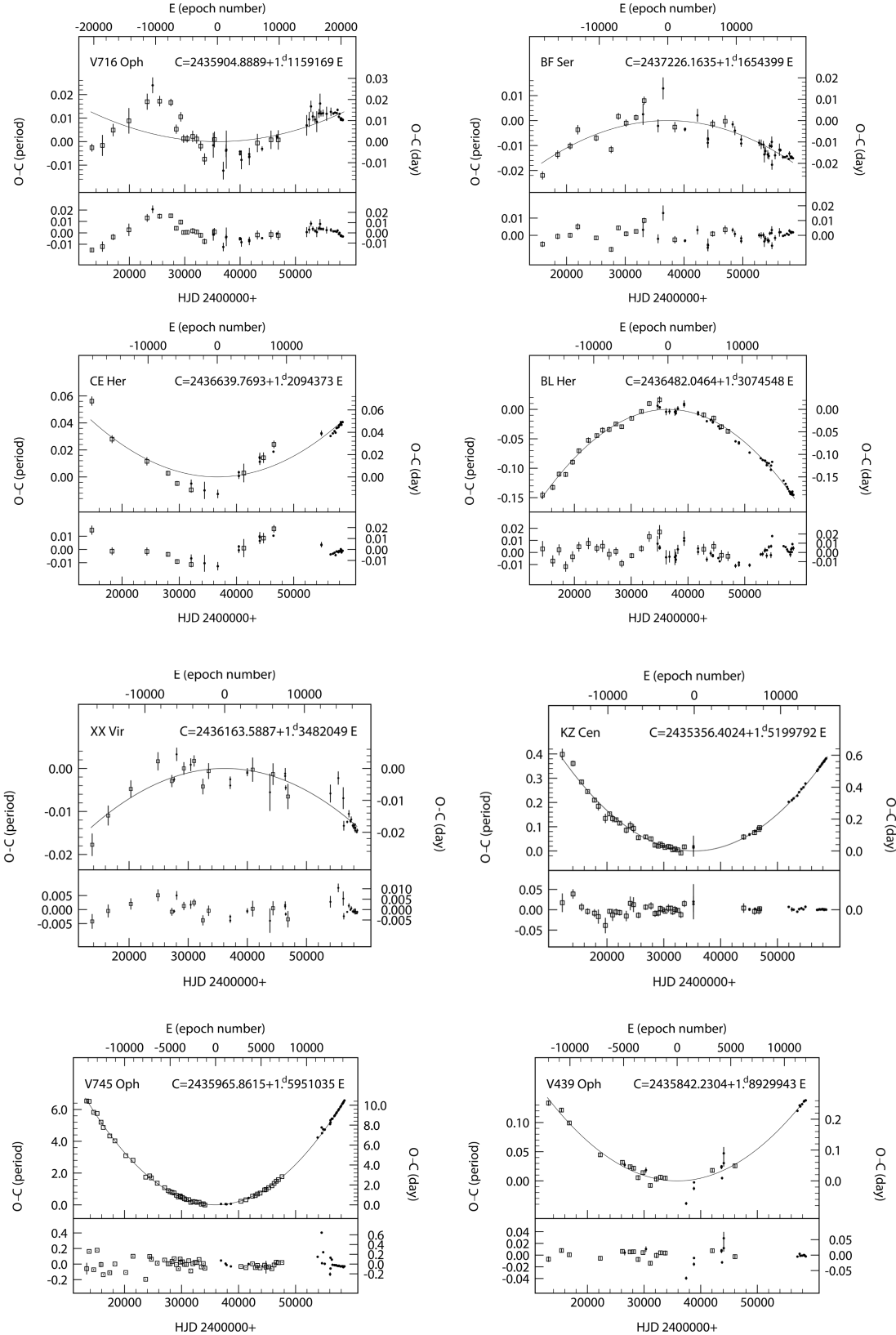


Figure 1. The $O - C$ diagrams for eight stars relative to the linear (top) and quadratic (bottom) elements (Table 4). The open squares represent the Harvard photographic observations, while dots are used for all other measurements; vertical bars indicating the limits of errors in the residuals.

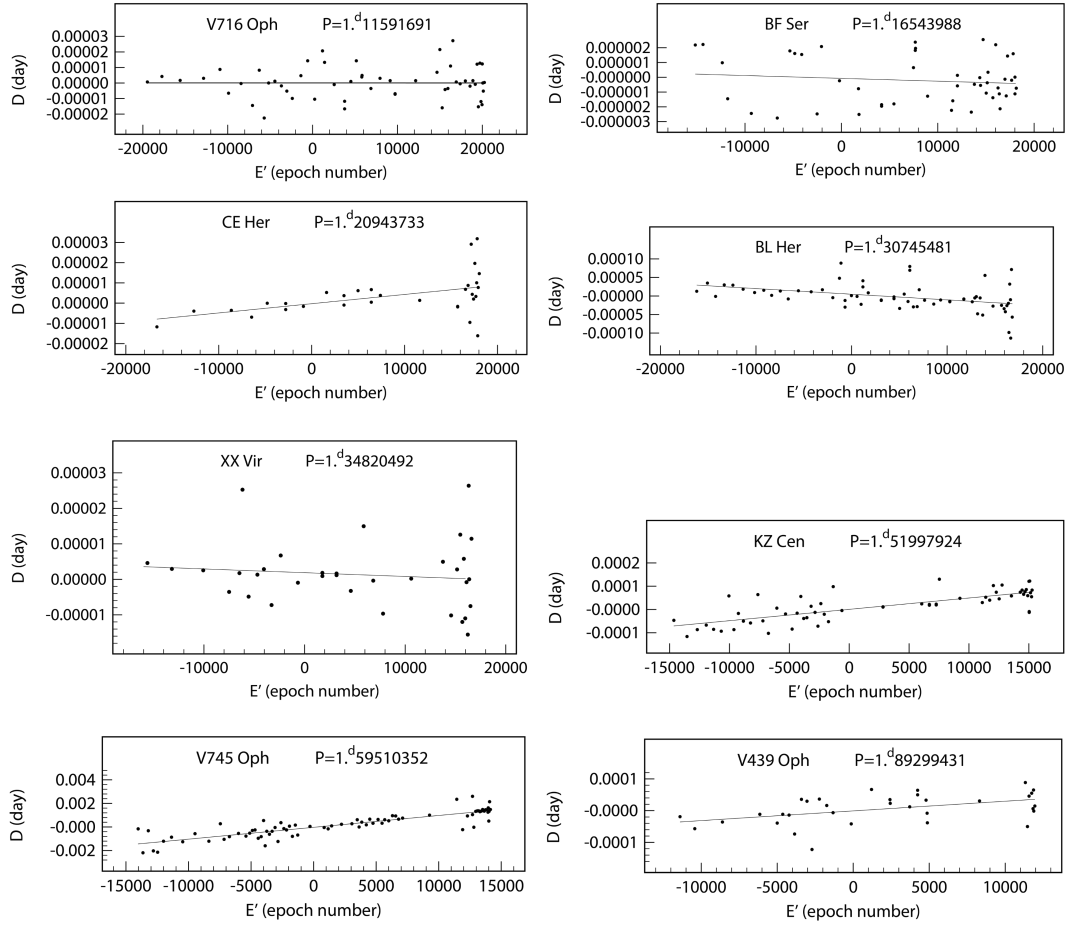


Figure 2. The period change in epoch interval (D_i) in days versus the epoch number (E'_i), showing the period change corresponding to the $O - C$ residuals.

3.2.2 Comparison with crossing times

Osborn et al. also estimated the crossing times, as a more quantitative method of comparing theory with observations, for stars evolving in the IS. Since the percentage of the crossing time spent in each evolutionary phase should correlate with the percentages of stars found in the sample, they calculated the proportion of the crossing time spent in each evolutionary phase (FRE, BE, and SRE). They compared this to the percentages of stars found in those stages in the sample, as presented in table 10 from Osborn et al. (2019). They found an absence of quantitative agreement between theory and observation, especially for BE stars. They speculated that this was due to their small sample size and proposed an in-depth examination of a larger sample of stars.

Although we have only 3 BE stars, that is more than Osborn et al. and our sample is large enough to compare crossing times quantitatively. Taking the 22 BLH stars from Table 6, where 14 are in SRE, 5 in FRE and 3 in BE crossing modes, the percentage of stars in each phase is 64% SRE, 23% FRE and 14% BE. These numbers can be compared with the theoretical values of 78%, 13% and 9% (Osborn et al. (2019) table 10, for the canonical $Y=0.25$). This is reasonable agreement given the sample size. Obviously a larger sample would allow a more precise comparison.

Table 5. The evolutionary crossing modes of the eight BLH stars based on the $dP/dt - P$ diagram of Osborn et al. (2019) illustrated in Fig 3

Stars	Period [d]	Rate of period change dP/dt [d/Myr]	Crossing modes
V716 Oph	1.1159169	0.022 ± 0.0048	SRE
BF Ser	1.1654399	-0.035 ± 0.0035	BE
CE Her	1.2094373	0.092 ± 0.0078	SRE
BL Her	1.3074548	-0.381 ± 0.0057	BE
XX Vir	1.3482049	-0.037 ± 0.0033	BE
KZ Cen	1.5199792	1.193 ± 0.0137	SRE
V745 Oph	1.5951035	23.987 ± 0.0891	FRE
V439 OPH	1.8929943	0.745 ± 0.0400	SRE

4 SUMMARY AND CONCLUSIONS

We investigate the period changes of eight BLH stars with periods between 1 and 2 days using all previously published data and all relevant observational survey data, including digitized photographic plates.

The $O - C$ diagrams for the stars studied show parabolic evolutionary trends, which indicate the presence of both increasing and decreasing periods for these BLHs over a baseline of more than a century. The derived period changes for such stars are in good agreement with the recent theoretical evolutionary framework proposed by

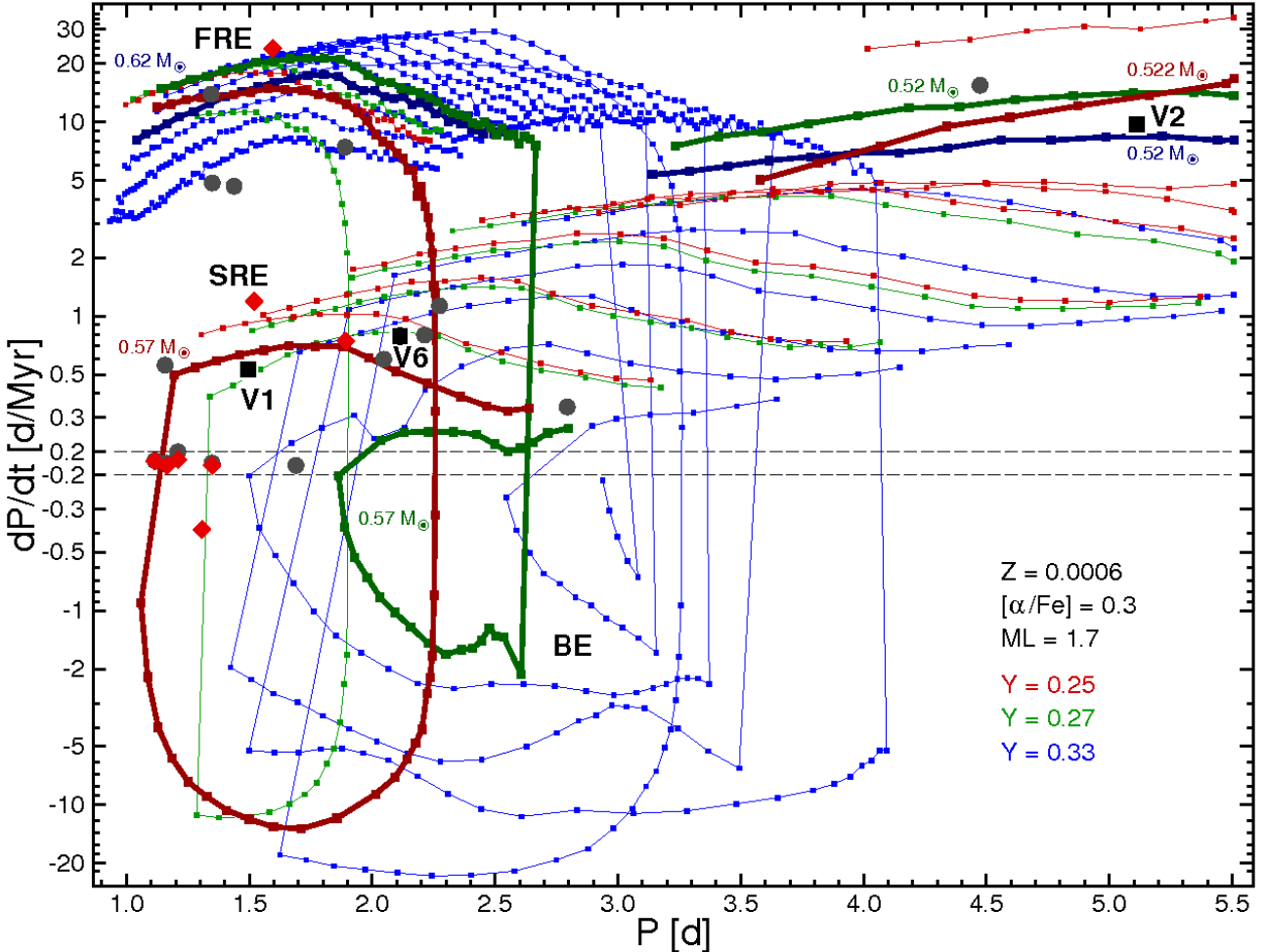


Figure 3. The theoretical rates of period change (dP/dt) as a function of period (P) for different masses (M) and helium abundances (Y), calculated from the Pisa stellar evolution models and taken from Osborn et al. (2019). They are over-plotted with the observed rate of period change of our BLH stars (red diamonds). Also shown are the period change rates of M13 V1, V2 and V6 (black squares), together with other T2Cs listed in Table 6 (gray circles). The ordinate shows the rate of change of the period, in days per million years, while the abscissa shows the pulsation period, in days. Models with $Y = 0.25$ are shown as red squares, with $Y = 0.27$ as green squares and with $Y = 0.33$ as blue ones. These models used α -elements enhancement $[\alpha/\text{Fe}] = +0.3$ and a mixing length parameter of $ML = 1.7$. Models for the same M and Y are connected by lines of the appropriate colour; the lines can be considered evolutionary tracks in the $P - dP/dt$ plane, and the regions corresponding to the three phases of evolution produced by loops are labelled FRE, BE and SRE. Tracks with masses corresponding to the M13 Cepheids are emphasised using thick lines labelled with mass, the labels having same colour as the appropriate track.

Bono et al. (2020), and with the Pisa group evolutionary tracks from Dell’Ommodarme et al. (2012) as presented by Osborn et al. (2019).

Our study found three BLH stars with decreasing periods, a significant increase over those reported by Gonzalez (1994). A more extensive study (in preparation) will further increase the number of BLH stars and improve the sample size for future studies.

We were able to determine the crossing mode of these stars by comparing with evolutionary tracks, as illustrated by Osborn et al. (2019). We found one star in FRE, four stars in SRE and three stars in BE crossing modes, respectively. The existence of decreasing periods for BLHs is important for the following reasons:

- It provides observational evidence for BE crossings with decreasing periods for BLHs, which were previously only known to have increasing periods and to be evolving redward.
- It fits with the recent theoretical evolutionary framework proposed by Bono et al. (2020).
- It supports the presence of GNLs predicted by Bono et al.

(1997a,b) and provides observational evidence for breathing pulse as suggested by Sweigart et al. (2000).

- The availability of a sample of BE stars provides quantitative agreement between theory and observation, especially for BE stars, thus the proportion of crossing times spent and the number of stars available in each evolutionary phase across the IS are approximately matched.

ACKNOWLEDGEMENTS

We thank the anonymous referee for valuable comments that improved the paper significantly. AMY acknowledges and thanks the South African Astronomical Observatory (SAAO) in Capetown, South Africa, and the Sternberg Astronomical Institute (SAI) of Moscow State University in Russia for the continuous support provided by research administrators and staff during his research visit.

Table 6. Published period changes of BLH stars, including the current work shown in Fig. 3, for comparison with Osborn et al. (2019)

Star	Period(P) [d]	Rate of period change(dP/dt) [d/Myr]	Error [d/Myr]	Years of span (ΔT) [yr]	Crossing modes	Source
V716 Oph	1.116	0.03[1]; 0.022[2]	0.0048 [2]	76 [1]; 129[2]	SRE	¹ Diethelm (1996); ² This paper
ω Cen V43	1.157	0.56	0.14	79	SRE	Jurcsik et al. (2001)
BF Ser	1.165	0.0[1]; -0.035[2]	0.0035	60[1]; 129[2]	BE	¹ Diethelm (1996); ² This paper
CE Her	1.209	0.2[1]; 0.092[2]	0.0078[2]	65[1]; 129[2]	SRE	¹ Diethelm (1996); ² This paper
BL Her	1.307	-0.381	0.0057	129	BE	This paper
ω Cen V92	1.345	13.94	0.56	100	FRE	Jurcsik et al. (2001)
XX Vir	1.348	0.0[1]; -0.037[2]	0.0033[2]	72[1]; 129[2]	BE	¹ Diethelm (1996); ² This paper
ω Cen V60	1.349	4.85	0.92	100	FRE	Jurcsik et al. (2001)
M15 V1	1.438	4.67	0.23	72	FRE	Wehlau & Bohlender (1982)
M13 V1	1.459	0.52	0.09	114	SRE	Osborn et al. (2019)
KZ Cen	1.519	1.193	0.0137	130	SRE	This paper
V745 Oph	1.595	23.987	0.0891	127	FRE	This paper
M22 V11	1.690	0.01	0.19	83	SRE	Wehlau & Bohlender (1982)
M14 V76	1.890	7.43	1.0	48	FRE	Wehlau & Froelich (1994)
V439 Oph	1.893	0.745	0.0400	131	SRE	This paper
EK Del	2.047	0.6	—	61	SRE	Diethelm (1990, 1996)
M13 V6	2.113	0.80	0.06	114	SRE	Osborn et al. (2019)
UY Eri	2.213	0.8	—	66	SRE	Diethelm (1996)
ω Cen V61	2.274	1.13	0.16	100	SRE	Jurcsik et al. (2001)
M14 V2	2.794	0.34	0.3	48	SRE	Wehlau & Froelich (1994)
ω Cen V48	4.474	15.45	—	79	SRE	Jurcsik et al. (2001)
M13 V2	5.111	9.2	0.7	115	SRE	Osborn et al. (2019)

AMY thanks and is indebted to Space Science and Geospatial Institute (SSGI) in Ethiopia for all financial and logistical support. AMY acknowledges and thanks Prof. Wayne Osborn from Central Michigan University, and Prof. Grzegorz Kopacki, from Wroclaw University Astronomical Institute, for providing the dP/dt - P diagram & information calculated from Pisa, stellar evolution model. This work makes use of the observational data available from the catalogue of Digital Access to a Sky Century at Harvard (DASCH), All Sky Automated Surveys (ASAS-3), All Sky Automated Surveys of SuperNovae (ASAS-SN), INTEGRAL-OMC, Catalina Sky Survey(CSS), PAN-STARSS, HIPPARCOS and data from Sternberg Astronomical Institute (SAI).

DATA AVAILABILITY

The data underlying this article are available in the article as well as the data source cited in the article and references therein.

REFERENCES

- Alexander A. L., Joner M. D., McNamara D. H., 1987, *PASP*, **99**, 645
Alfonso-Garzón J., Domingo A., Mas-Hesse J. M., Giménez A., 2012, *A&A*, **548**, A79
Arellano Ferro A., Rojo Arellano E., González-Bedolla S., Rosenzweig P., 1998, *ApJS*, **117**, 167
Arp H. C., 1955, *AJ*, **60**, 1
Ashbrook J., 1950, *AJ*, **55**, 62
Berdnikov L. N., 1992, Soviet Astronomy Letters, **18**, 207
Bhardwaj A., 2022, *Universe*, **8**, 122
Bono G., Caputo F., Cassisi S., Castellani V., Marconi M., 1997a, *ApJ*, **479**, 279
Bono G., Caputo F., Cassisi S., Castellani V., Marconi M., 1997b, *ApJ*, **489**, 822
Bono G., et al., 2016, Communications of the Konkoly Observatory Hungary, **105**, 149
Bono G., et al., 2020, *A&A*, **644**, A96
Bookmeyer B. B., Fitch W. S., Lee T. A., Wisniewski W. Z., Johnson H. L., 1977, *Rev. Mex. Astron. Astrofis.*, **2**, 235
Catelan M., Smith H. A., 2015, Pulsating Stars
Chambers K. C., et al., 2016, arXiv e-prints, p. [arXiv:1612.05560](https://arxiv.org/abs/1612.05560)
Christianson J., 1983, Journal of the American Association of Variable Star Observers, **12**, 54
Constantino T., Campbell S. W., Lattanzio J. C., van Duijneveldt A., 2016, *MNRAS*, **456**, 3866
Dell’Omodarme M., Valle G., Degl’Innocenti S., Prada Moroni P. G., 2012, *A&A*, **540**, A26
Diethelm R., 1983, *A&A*, **124**, 108
Diethelm R., 1986, *A&AS*, **64**, 261
Diethelm R., 1990, *A&A*, **239**, 186
Diethelm R., 1996, *A&A*, **307**, 803
Diethelm R., Tamman G. A., 1982, *A&AS*, **47**, 335
Dotter A., 2008, *ApJ*, **687**, L21
Drake A. J., et al., 2013, *ApJ*, **765**, 154
Eddington A. S., Plakidis S., 1929, *MNRAS*, **90**, 65
Gingold R. A., 1976, *ApJ*, **204**, 116
Gingold R. A., 1985, *Mem. Soc. Astron. Italiana*, **56**, 169
Gonzalez G., 1994, *AJ*, **108**, 1312
Grindlay J., Tang S., Los E., Servillat M., 2012, in Griffin E., Hanisch R., Seaman R., eds, Vol. 285, New Horizons in Time Domain Astronomy. pp 29–34 ([arXiv:1211.1051](https://arxiv.org/abs/1211.1051)), doi:10.1017/S1743921312000166
Harris H. C., 1980, PhD thesis, University of Washington, Seattle
Henden A. A., 1980, *MNRAS*, **192**, 621
Henden A. A., 1996, *AJ*, **112**, 2757
Hertzsprung E., 1919, *Astronomische Nachrichten*, **210**, 17
Ignatova V. V., Vozyakova O. V., 2000, *Astronomical and Astrophysical Transactions*, **19**, 133
Irwin J. B., 1961, *ApJS*, **6**, 253
Jurcsik J., Clement C., Geyer E. H., Domka I., 2001, *AJ*, **121**, 951
Kinman T. D., 1965, *ApJ*, **142**, 655
Kinman T. D., Wong-Swanson B., Wenz M., Harlan E. A., 1984, *AJ*, **89**, 1200
Kochanek C. S., et al., 2017, *PASP*, **129**, 104502
Kwee K. K., Diethelm R., 1984, *A&AS*, **55**, 77
Lin C. C., 1983, in Athanassoula E., ed., Vol. 100, Internal Kinematics and

- Dynamics of Galaxies. p. 117
- Lombard F., Koen C., 1993, *MNRAS*, **263**, 309
- Loomis C., Schmidt E. G., Simon N. R., 1988, *MNRAS*, **235**, 1059
- Mandel O. E., 1970, *Peremennye Zvezdy*, **17**, 347
- McNamara D. H., Pyne M. D., 1994, *PASP*, **106**, 472
- Meakes M., Wallerstein G., Opalko J. F., 1991, *AJ*, **101**, 1795
- Michałowska-Smak A., Smak J., 1965, *Acta Astron.*, **15**, 333
- Mitchell R. I., Iriarte B., Steinmetz D., Johnson H. L., 1964, *Boletin de los Observatorios Tonantzintla y Tacubaya*, **3**, 153
- Moffett T. J., Barnes T. G. I., 1984, *ApJS*, **55**, 389
- Neilson H. R., Percy J. R., Smith H. A., 2016, *Journal of the American Association of Variable Star Observers*, **44**, 179
- Nikulina T. G., 1966, *Bull. Inst. Astrophys.*, **46**, 15
- Oosterhoff P. T., 1936, *Bull. Astron. Inst. Netherlands*, **8**, 41
- Osborn W., 1969, *AJ*, **74**, 108
- Osborn W., Kopacki G., Smith H. A., Layden A., Pritzl B., Kuehn C., Anderson M., 2019, *Acta Astron.*, **69**, 101
- Perryman M. A. C., et al., 1997, *A&A*, **323**, L49
- Petersen J. O., Hansen L., 1984, *A&A*, **134**, 319
- Pojmanski G., 2002, *Acta Astron.*, **52**, 397
- Preston G. W., Kilstrom S. D., 1967, *ApJ*, **148**, 787
- Provencal J., 1986, *Journal of the American Association of Variable Star Observers*, **15**, 36
- Samus' N. N., Kazarovets E. V., Durlevich O. V., Kireeva N. N., Pastukhova E. N., 2017, *Astronomy Reports*, **61**, 80
- Sandage A., Diethelm R., Tammann G. A., 1994, *A&A*, **283**, 111
- Smith H. A., 2013, arXiv e-prints, p. [arXiv:1310.0533](https://arxiv.org/abs/1310.0533)
- Smolec R., 2016, *MNRAS*, **456**, 3475
- Soloviev A. W., 1952, *Peremennye Zvezdy*, **9**, 101
- Soszyński I., et al., 2018, *Acta Astron.*, **68**, 89
- Sterken C., 2005, in Sterken C., ed., *Astronomical Society of the Pacific Conference Series Vol. 335, The Light-Time Effect in Astrophysics: Causes and cures of the O-C diagram*. p. 3
- Sturch C., 1966, *PASP*, **78**, 210
- Sweigart A. V., Lattanzio J. C., Gray J. P., Tout C. A., 2000, in Noels A., Magain P., Caro D., Jehin E., Parmentier G., Thoul A. A., eds, Liege International Astrophysical Colloquia Vol. 35, Liege International Astrophysical Colloquia. p. 529 ([arXiv:astro-ph/9909404](https://arxiv.org/abs/astro-ph/9909404))
- Szabados L., 1977, *Mitt. Sternw. Ungarisch. Akad. Wiss.*, **70**
- Tsesevich V. P., 1952, *Peremennye Zvezdy*, **2**, 116
- Wallerstein G., 2002, *PASP*, **114**, 689
- Wehlau A., Bohlender D., 1982, *AJ*, **87**, 780
- Wehlau A., Froelich N., 1994, *AJ*, **108**, 134

APPENDIX A: SUPPLEMENTARY MATERIALS

A1 Times of maximum light

The results of reduction of the seasonal light-curves for all stars are presented in Table A1. Columns 1, 2 and 3 give the times of maximum light and their errors; column 4 gives the type of observations used; columns 5 and 6 contain the epoch number (E) and the $O - C$ residual; columns 7 and 8 contain the number of observations (N) and the data sources, respectively.

Table A1: Times of maximum light

Max, HJD	Year	Uncertainty	Filter	E	O–C, days	N	Reference
V716 Oph							
2413238.3811	1895-02-13	0.0018	PG	-20312	-0.0028	31	DASCH
2415142.1364	1900-05-02	0.0050	PG	-18606	-0.0017	69	DASCH
2417078.2595	1905-08-20	0.0030	PG	-16871	0.0055	106	DASCH
2419917.1566	1913-05-29	0.0061	PG	-14327	0.0099	92	DASCH
2423221.3956	1922-06-15	0.0038	PG	-11366	0.0190	95	DASCH
2424211.2217	1925-03-01	0.0037	PG	-10479	0.0268	45	Lin (1983)
2425483.3594	1928-08-24	0.0025	PG	-9339	0.0193	122	DASCH
2427502.0525	1934-03-05	0.0018	PG	-7530	0.0186	196	DASCH
2428479.5831	1936-11-07	0.0022	PG	-6654	0.0060	89	DASCH
2429280.8172	1939-01-17	0.0023	PG	-5936	0.0118	162	DASCH
2429795.2446	1940-06-14	0.0019	PG	-5475	0.0014	133	DASCH
2430436.8968	1942-03-18	0.0018	PG	-4900	0.0014	190	DASCH
2431442.3390	1944-12-17	0.0027	PG	-3999	0.0025	151	DASCH
2432153.1769	1946-11-28	0.0022	PG	-3362	0.0013	168	DASCH
2432886.3309	1948-11-30	0.0023	PG	-2705	-0.0021	120	DASCH
2433587.1205	1950-11-01	0.0027	PG	-2077	-0.0083	80	DASCH
2435157.2222	1955-02-18	0.0059	PG	-670	-0.0017	25	Mandel (1970)
2435370.3651	1955-09-19	0.0037	PG	-479	0.0010	25	DASCH
2436961.6478	1960-01-28	0.0042	PG	947	-0.0137	32	SAI (this paper)
2437470.5153	1961-06-20	0.0030	PG	1403	-0.0043	33	Kinman (1965)
2437514.0366	1961-08-02	0.0091	PG	1442	-0.0038	57	Mandel (1970)
2439977.9790	1968-05-01	0.0007	B	3650	-0.0059	38	Bookmeyer et al. (1977)
2439977.9808	1968-05-01	0.0007	V	3650	-0.0047	38	Bookmeyer et al. (1977)
2440237.9849	1969-01-16	0.0044	PG	3883	-0.0086	24	SAI (this paper)
2441639.5786	1972-11-18	0.0006	V	5139	-0.0073	49	Kwee & Diethelm (1984)
2441639.5793	1972-11-18	0.0004	B	5139	-0.0059	49	Kwee & Diethelm (1984)
2441663.0125	1972-12-11	0.0041	PG	5160	-0.0070	59	SAI (this paper)
2443129.3337	1976-12-16	0.0044	PG	6474	-0.0006	67	DASCH
2443985.2392	1979-04-21	0.0012	PG	7241	-0.0034	34	Kinman (1965)
2445581.0046	1983-09-03	0.0044	PG	8671	0.0009	43	DASCH
2446646.7067	1986-08-04	0.0011	B	9626	0.0023	78	McNamara & Pyne (1994)
2446646.7075	1986-08-04	0.0012	V	9626	0.0024	78	McNamara & Pyne (1994)
2446893.3229	1987-04-07	0.0046	PG	9847	0.0008	71	DASCH
2452032.1278	2001-05-02	0.0049	V	14452	0.0077	47	ASAS-3
2452479.6133	2002-07-24	0.0036	V	14853	0.0105	22	ASAS-3
2452801.0035	2003-06-10	0.0027	V	15141	0.0167	68	ASAS-3
2453134.6579	2004-05-09	0.0023	V	15440	0.0119	43	ASAS-3
2453533.0388	2005-06-11	0.0016	V	15797	0.0105	68	ASAS-3
2453848.8423	2006-04-23	0.0049	V	16080	0.0095	35	ASAS-3
2454252.8081	2007-06-01	0.0021	V	16442	0.0134	76	ASAS-3
2454443.6346	2007-12-09	0.0047	V	16613	0.0180	212	CSS
2454612.1333	2008-05-25	0.0014	V	16764	0.0133	94	ASAS-3
2454983.7338	2009-06-01	0.0016	V	17097	0.0135	51	ASAS-3
2455623.1539	2011-03-02	0.0034	V	17670	0.0132	117	CSS
2456396.4852	2013-04-13	0.0020	V	18363	0.0141	62	ASAS-SN
2456837.2716	2014-06-28	0.0007	V	18758	0.0133	117	ASAS-SN
2457148.6129	2015-05-06	0.0003	V	19037	0.0137	193	ASAS-SN
2457457.7216	2016-03-10	0.0004	V	19314	0.0135	125	ASAS-SN
2457599.4446	2016-07-29	0.0007	V	19441	0.0150	100	ASAS-SN
2457837.1316	2017-03-24	0.0007	V	19654	0.0118	100	ASAS-SN
2457956.5361	2017-07-22	0.0005	V	19761	0.0131	108	ASAS-SN
2458159.6261	2018-02-10	0.0002	g	19943	0.0063	120	ASAS-SN
2458212.0735	2018-04-03	0.0006	g	19990	0.0056	100	ASAS-SN
2458262.2951	2018-05-23	0.0008	V	20035	0.0109	139	ASAS-SN
2458295.7679	2018-06-26	0.0003	g	20065	0.0062	100	ASAS-SN
2458428.5614	2018-11-06	0.0004	g	20184	0.0055	100	ASAS-SN

Table A1 – *Continued*

Max, HJD	Year	Uncertainty	Filter	E	O–C, days	N	Reference
2458572.5147	2019-03-30	0.0007	<i>g</i>	20313	0.0056	83	ASAS-SN
BF Ser							
2415910.2467	1902-06-09	0.0019	<i>PG</i>	-18290	-0.0247	87	DASCH
2418492.8713	1909-07-05	0.0020	<i>PG</i>	-16074	-0.0149	115	DASCH
2420613.9758	1915-04-26	0.0016	<i>PG</i>	-14254	-0.0110	145	DASCH
2421911.1180	1918-11-13	0.0022	<i>PG</i>	-13141	-0.0034	131	DASCH
2425049.6437	1927-06-18	0.0015	<i>PG</i>	-10448	-0.0073	145	DASCH
2427593.7936	1934-06-05	0.0017	<i>PG</i>	-8265	-0.0126	168	DASCH
2428828.0099	1937-10-21	0.0016	<i>PG</i>	-7206	0.0029	210	DASCH
2430147.2848	1941-06-01	0.0017	<i>PG</i>	-6074	-0.0002	166	DASCH
2431831.3479	1946-01-10	0.0014	<i>PG</i>	-4629	0.0023	164	DASCH
2433011.9401	1949-04-05	0.0050	<i>PG</i>	-3616	0.0039	29	Nikulina (1966)
2433214.7330	1949-10-25	0.0019	<i>PG</i>	-3442	0.0102	182	DASCH
2435577.0678	1956-04-13	0.0030	<i>PG</i>	-1415	-0.0016	64	Nikulina (1966)
2436439.5109	1958-08-24	0.0051	<i>PG</i>	-675	0.0160	29	Mandel (1970)
2438431.2295	1964-02-05	0.0024	<i>PG</i>	1034	-0.0021	114	DASCH
2440154.9139	1968-10-25	0.0009	<i>B</i>	2513	-0.0033	72	Bookmeyer et al. (1977)
2440160.7372	1968-10-31	0.0006	<i>V</i>	2518	-0.0029	74	Bookmeyer et al. (1977)
2442287.6756	1974-08-28	0.0030	<i>PG</i>	4343	0.0034	53	SAI (this paper)
2444039.3146	1979-06-14	0.0020	<i>V</i>	5846	-0.0095	12	Harris (1980)
2444068.4526	1979-07-13	0.0041	<i>V</i>	5871	-0.0074	19	Diethelm & Tamman (1982)
2444069.6219	1979-07-15	0.0040	<i>B</i>	5872	-0.0079	18	Diethelm & Tamman (1982)
2444872.6172	1981-09-25	0.0019	<i>PG</i>	6561	-0.0006	155	DASCH
2446997.2153	1987-07-20	0.0029	<i>PG</i>	8384	0.0006	70	DASCH
2448285.0207	1991-01-28	0.0016	<i>V</i>	9489	-0.0008	64	Hipparcos
2448652.1313	1992-01-30	0.0021	<i>V</i>	9804	-0.0038	61	Hipparcos
2449726.6609	1995-01-09	0.0016	<i>V</i>	10726	-0.0098	22	Henden (1996)
2449726.6670	1995-01-09	0.0019	<i>B</i>	10726	-0.0079	22	Henden (1996)
2452773.1211	2003-05-13	0.0016	<i>V</i>	13340	-0.0094	60	ASAS-3
2453120.4214	2004-04-24	0.0022	<i>V</i>	13638	-0.0102	37	ASAS-3
2453506.1819	2005-05-15	0.0017	<i>V</i>	13969	-0.0103	58	ASAS-3
2453668.1734	2005-10-24	0.0037	<i>V</i>	14108	-0.0149	44	CSS
2453855.8108	2006-04-30	0.0018	<i>V</i>	14269	-0.0133	37	ASAS-3
2454245.0662	2007-05-24	0.0020	<i>V</i>	14603	-0.0149	45	ASAS-3
2454419.8814	2007-11-15	0.0016	<i>V</i>	14753	-0.0156	71	CSS
2454608.6875	2008-05-22	0.0013	<i>V</i>	14915	-0.0108	62	ASAS-3
2454881.4002	2009-02-18	0.0008	<i>V</i>	15149	-0.0111	132	INTEGRAL-OMC
2454932.6815	2009-04-11	0.0025	<i>V</i>	15193	-0.0090	47	CSS
2454962.9723	2009-05-11	0.0023	<i>V</i>	15219	-0.0197	35	ASAS-3
2455497.9136	2010-10-28	0.0019	<i>V</i>	15678	-0.0153	68	CSS
2456229.8125	2012-10-29	0.0029	<i>V</i>	16306	-0.0127	84	CSS
2456416.2827	2013-05-03	0.0007	<i>V</i>	16466	-0.0129	70	ASAS-SN
2456845.1613	2014-07-06	0.0008	<i>V</i>	16834	-0.0161	140	ASAS-SN
2457156.3337	2015-05-13	0.0004	<i>V</i>	17101	-0.0162	143	ASAS-SN
2457510.6279	2016-05-02	0.0005	<i>V</i>	17405	-0.0157	260	ASAS-SN
2457813.6409	2017-03-01	0.0004	<i>V</i>	17665	-0.0170	120	ASAS-SN
2457926.6911	2017-06-22	0.0011	<i>V</i>	17762	-0.0145	90	ASAS-SN
2458148.1151	2018-01-29	0.0004	<i>g</i>	17952	-0.0241	120	ASAS-SN
2458212.2137	2018-04-03	0.0003	<i>g</i>	18007	-0.0247	100	ASAS-SN
2458233.1998	2018-04-24	0.0006	<i>V</i>	18025	-0.0165	171	ASAS-SN
2458307.7802	2018-07-08	0.0004	<i>g</i>	18089	-0.0243	130	ASAS-SN
2458543.1984	2019-02-28	0.0004	<i>g</i>	18291	-0.0249	155	ASAS-SN
CE Her							
2414721.2099	1899-03-07	0.0041	<i>PG</i>	-18123	0.0680	59	DASCH
2418255.1516	1908-11-09	0.0035	<i>PG</i>	-15201	0.0338	159	DASCH
2424349.4865	1925-07-17	0.0037	<i>PG</i>	-10162	0.0140	181	DASCH
2428028.5842	1935-08-14	0.0022	<i>PG</i>	-7120	0.0033	213	DASCH
2429626.2417	1939-12-28	0.0022	<i>PG</i>	-5799	-0.0059	198	DASCH

Table A1 – *Continued*

Max, HJD	Year	Uncertainty	Filter	E	O–C, days	N	Reference
2432087.4413	1946-09-23	0.0036	VIS	-3764	-0.0059	122	Mandel (1970)
2432091.0693	1946-09-27	0.0026	PG	-3761	-0.0116	385	DASCH
2434408.3507	1953-01-30	0.0077	PG	-1845	-0.0121	33	Mandel (1970)
2436732.8861	1959-06-13	0.0038	PG	77	-0.0153	88	Mandel (1970)
2440410.7957	1969-07-08	0.0027	V	3118	0.0008	26	Bookmeyer et al. (1977)
2440410.8044	1969-07-08	0.0014	B	3118	0.0042	26	Bookmeyer et al. (1977)
2441280.3892	1971-11-24	0.0083	PG	3837	0.0035	121	DASCH
2444043.9623	1979-06-19	0.0026	V	6122	0.0176	11	Harris (1980)
2444070.5692	1979-07-16	0.0049	V	6144	0.0169	25	Diethelm & Tammann (1982)
2444070.5712	1979-07-16	0.0029	B	6144	0.0136	25	Diethelm & Tammann (1982)
2444717.6238	1981-04-23	0.0047	PG	6679	0.0172	68	DASCH
2446461.6325	1986-01-31	0.0003	V	8121	0.0227	127	Loomis et al. (1988)
2446543.8861	1986-04-23	0.0034	PG	8189	0.0291	155	DASCH
2454840.6304	2009-01-09	0.0018	V	15049	0.0387	117	INTEGRAL-OMC
2454851.5157	2009-01-20	0.0024	V	15058	0.0391	101	CSS
2456450.3894	2013-06-06	0.0010	V	16380	0.0367	111	ASAS-SN
2456854.3438	2014-07-15	0.0003	V	16714	0.0390	122	ASAS-SN
2457136.1447	2015-04-23	0.0003	V	16947	0.0410	100	ASAS-SN
2457316.3495	2015-10-20	0.0005	V	17096	0.0396	100	ASAS-SN
2457486.8843	2016-04-08	0.0004	V	17237	0.0437	100	ASAS-SN
2457606.6190	2016-08-06	0.0004	V	17336	0.0441	121	ASAS-SN
2457830.3652	2017-03-17	0.0005	V	17521	0.0445	100	ASAS-SN
2457930.7502	2017-06-26	0.0005	V	17604	0.0461	99	ASAS-SN
2458106.1191	2017-12-18	0.0006	V	17749	0.0466	99	ASAS-SN
2458143.6141	2018-01-25	0.0003	g	17780	0.0490	100	ASAS-SN
2458228.2769	2018-04-19	0.0004	g	17850	0.0513	100	ASAS-SN
2458281.4914	2018-06-11	0.0005	g	17894	0.0505	99	ASAS-SN
2458329.8671	2018-07-30	0.0005	V	17934	0.0487	111	ASAS-SN
2458360.1031	2018-08-29	0.0005	g	17959	0.0488	119	ASAS-SN
2458559.6627	2019-03-17	0.0005	g	18124	0.0512	117	ASAS-SN
BL Her							
2414401.5576	1898-04-22	0.0085	PG	-16888	-0.1912	66	DASCH
2416207.1700	1903-04-02	0.0061	PG	-15507	-0.1739	253	DASCH
2417308.0764	1906-04-07	0.0059	PG	-14665	-0.1444	197	DASCH
2418474.3252	1909-06-16	0.0056	PG	-13773	-0.1452	197	DASCH
2419687.6708	1912-10-12	0.0060	PG	-12845	-0.1177	186	DASCH
2420805.5699	1915-11-04	0.0052	PG	-11990	-0.0924	271	DASCH
2422471.2907	1920-05-26	0.0062	PG	-10716	-0.0691	205	DASCH
2423963.1071	1924-06-26	0.0046	PG	-9575	-0.0587	220	DASCH
2424960.7070	1927-03-21	0.0064	PG	-8812	-0.0468	134	DASCH
2426129.5730	1930-06-02	0.0061	PG	-7918	-0.0453	197	DASCH
2427320.6767	1933-09-05	0.0044	PG	-7007	-0.0330	278	DASCH
2428340.4854	1936-06-20	0.0042	PG	-6227	-0.0390	294	DASCH
2430102.9532	1941-04-18	0.0027	PG	-4879	-0.0204	693	DASCH
2431806.5820	1945-12-17	0.0035	PG	-3576	-0.0052	508	DASCH
2433178.1195	1949-09-18	0.0057	PG	-2527	0.0122	277	DASCH
2434639.8492	1953-09-19	0.0084	PG	-1409	0.0075	59	Mandel (1970)
2435000.7199	1954-09-15	0.0075	PG	-1133	0.0207	130	DASCH
2435017.6993	1954-10-02	0.0015	B	-1120	0.0031	124	Mitchell et al. (1964)
2435034.6988	1954-10-19	0.0023	V	-1107	0.0049	125	Mitchell et al. (1964)
2436157.7909	1957-11-15	0.0078	PG	-248	-0.0059	111	Mandel (1970)
2436744.8402	1959-06-25	0.0063	PGV	201	-0.0047	87	Mandel (1970)
2437699.2797	1962-02-03	0.0087	PG	931	-0.0062	65	Mandel (1970)
2437873.1682	1962-07-27	0.0036	B	1064	-0.0092	25	Michałowska-Smak & Smak (1965)
2437873.1740	1962-07-27	0.0041	V	1064	-0.0043	25	Michałowska-Smak & Smak (1965)
2438218.3485	1963-07-07	0.0049	PGV	1328	0.0021	122	Mandel (1970)
2438218.3485	1963-07-07	0.0049	PGV	1328	0.0021	122	Mandel (1970)
2439325.7700	1966-07-19	0.0054	V	2175	0.0094	48	Preston & Kilstrom (1967)

Table A1 – *Continued*

Max, HJD	Year	Uncertainty	Filter	E	O–C, days	N	Reference
2439325.7715	1966-07-19	0.0076	B	2175	0.0118	48	Preston & Kilstom (1967)
2441788.9933	1973-04-16	0.0033	B	4059	-0.0113	23	Szabados (1977)
2441788.9986	1973-04-16	0.0038	V	4059	-0.0069	23	Szabados (1977)
2442774.8126	1975-12-28	0.0058	PG	4813	-0.0129	67	DASCH
2443322.6237	1977-06-28	0.0028	V	5232	-0.0262	28	Alexander et al. (1987)
2444014.2700	1979-05-20	0.0032	V	5761	-0.0236	14	Harris (1980)
2444381.6592	1980-05-22	0.0009	B	6042	-0.0283	69	Moffett & Barnes (1984)
2444381.6594	1980-05-22	0.0007	V	6042	-0.0290	69	Moffett & Barnes (1984)
2444541.1771	1980-10-28	0.0054	PG	6164	-0.0199	79	DASCH
2445355.7032	1983-01-21	0.0008	B	6787	-0.0381	271	Alexander et al. (1987)
2445589.7339	1983-09-12	0.0008	V	6966	-0.0427	243	Alexander et al. (1987)
2445906.1406	1984-07-24	0.0057	PG	7208	-0.0391	74	DASCH
2447044.9237	1987-09-06	0.0051	PG	8079	-0.0492	79	DASCH
2448373.2769	1991-04-26	0.0022	V	9095	-0.0710	123	HIPPARCOS
2448973.3938	1992-12-16	0.0019	V	9554	-0.0759	30	Arellano Ferro et al. (1998)
2448973.3948	1992-12-16	0.0014	B	9554	-0.0739	30	Arellano Ferro et al. (1998)
2450846.9550	1998-02-02	0.0014	B	10987	-0.0965	36	Ignatova & Vozyakova (2000)
2450846.9562	1998-02-02	0.0021	V	10987	-0.0962	36	Ignatova & Vozyakova (2000)
2452817.2783	2003-06-26	0.0017	V	12494	-0.1085	57	ASAS-3
2453146.7530	2004-05-21	0.0025	V	12746	-0.1124	32	ASAS-3
2453518.0686	2005-05-27	0.0020	V	13030	-0.1140	34	ASAS-3
2453588.6711	2005-08-06	0.0024	V	13084	-0.1141	31	ASAS-3
2453859.3043	2006-05-03	0.0029	V	13291	-0.1240	27	ASAS-3
2453898.5334	2006-06-12	0.0009	V	13321	-0.1186	191	ASAS-3
2454248.9298	2007-05-28	0.0021	V	13589	-0.1200	30	ASAS-3
2454607.1584	2008-05-20	0.0031	V	13863	-0.1340	26	ASAS-3
2454641.1614	2008-06-23	0.0017	V	13889	-0.1249	56	ASAS-3
2454834.6730	2009-01-03	0.0013	V	14037	-0.1166	54	INTEGRAL-OMC
2456829.8073	2014-06-21	0.0009	V	15563	-0.1583	197	ASAS-SN
2457199.8099	2015-06-26	0.0010	V	15846	-0.1654	167	ASAS-SN
2457463.9088	2016-03-16	0.0014	V	16048	-0.1723	100	ASAS-SN
2457601.1871	2016-07-31	0.0010	V	16153	-0.1768	152	ASAS-SN
2457865.2877	2017-04-21	0.0009	V	16355	-0.1821	150	ASAS-SN
2457992.1089	2017-08-26	0.0011	V	16452	-0.1840	89	ASAS-SN
2458041.7941	2017-10-15	0.0029	g	16490	-0.1821	44	ASAS-SN
2458176.4653	2018-02-26	0.0014	g	16593	-0.1788	95	ASAS-SN
2458239.2226	2018-04-30	0.0017	g	16641	-0.1793	96	ASAS-SN
2458290.2033	2018-06-20	0.0009	V	16680	-0.1894	161	ASAS-SN
2458334.6661	2018-08-04	0.0012	g	16714	-0.1800	99	ASAS-SN
2458392.1973	2018-09-30	0.0014	g	16758	-0.1768	87	ASAS-SN
2458564.7738	2019-03-22	0.0024	g	16890	-0.1844	90	ASAS-SN
XX Vir							
2413761.7782	1896-07-21	0.0035	PG	-16616	-0.0239	24	DASCH
2416467.6346	1903-12-19	0.0031	PG	-14609	-0.0148	100	DASCH
2420293.8485	1914-06-10	0.0027	PG	-11771	-0.0064	114	DASCH
2424887.1914	1927-01-06	0.0029	PG	-8364	0.0022	138	DASCH
2427227.6690	1933-06-04	0.0019	PG	-6628	-0.0040	185	DASCH
2427632.1310	1934-07-13	0.0007	PG	-6328	-0.0034	329	Oosterhoff (1936)
2429264.8106	1939-01-01	0.0020	PG	-5117	0.0000	310	DASCH
2430435.0536	1942-03-16	0.0020	PG	-4249	0.0011	80	Mandel (1970)
2430997.2563	1943-09-29	0.0018	PG	-3832	0.0023	295	DASCH
2432480.2737	1947-10-21	0.0025	PG	-2732	-0.0057	115	DASCH
2433450.9861	1950-06-18	0.0025	PG	-2012	-0.0008	90	DASCH
2437107.3153	1960-06-21	0.0009	B	700	-0.0034	42	Mitchell et al. (1964)
2437107.3268	1960-06-21	0.0011	V	700	-0.0054	42	Mitchell et al. (1964)
2439997.8686	1968-05-21	0.0004	B	2844	-0.0015	25	Bookmeyer et al. (1977)
2439997.8824	1968-05-21	0.0013	V	2844	-0.0012	25	Bookmeyer et al. (1977)
2440895.7741	1970-11-05	0.0038	PG	3510	-0.0004	25	DASCH

Table A1 – *Continued*

Max, HJD	Year	Uncertainty	Filter	E	O–C, days	N	Reference
2443826.7780	1978-11-14	0.0059	V	5684	-0.0075	8	Harris (1980)
2444340.4364	1980-04-10	0.0034	PG	6065	-0.0018	114	DASCH
2446404.5375	1985-12-05	0.0015	B	7596	-0.0024	61	McNamara & Pyne (1994)
2446404.5517	1985-12-05	0.0018	V	7596	-0.0016	61	McNamara & Pyne (1994)
2446482.7432	1986-02-21	0.0008	V	7654	-0.0060	76	Loomis et al. (1988)
2446866.9654	1987-03-12	0.0039	PG	7939	-0.0088	67	DASCH
2454050.2157	2006-11-10	0.0028	V	13267	-0.0079	101	CSS
2455379.5506	2010-07-02	0.0021	V	14253	-0.0030	92	CSS
2456214.0831	2012-10-13	0.0034	V	14872	-0.0093	62	CSS
2456313.8416	2013-01-21	0.0015	V	14946	-0.0180	57	ASAS-SN
2456900.3120	2014-08-30	0.0004	V	15381	-0.0168	170	ASAS-SN
2457175.3484	2015-06-01	0.0011	V	15585	-0.0142	128	ASAS-SN
2457435.5496	2016-02-17	0.0005	V	15778	-0.0165	110	ASAS-SN
2457569.0225	2016-06-29	0.0009	V	15877	-0.0160	103	ASAS-SN
2457810.3492	2017-02-25	0.0005	V	16056	-0.0179	111	ASAS-SN
2457922.2501	2017-06-17	0.0009	V	16139	-0.0180	118	ASAS-SN
2458139.3023	2018-01-20	0.0008	g	16300	-0.0268	110	ASAS-SN
2458191.8833	2018-03-14	0.0004	g	16339	-0.0258	110	ASAS-SN
2458249.8624	2018-05-11	0.0006	V	16382	-0.0195	161	ASAS-SN
2458280.8638	2018-06-11	0.0004	g	16405	-0.0268	162	ASAS-SN
2458508.7091	2019-01-25	0.0004	g	16574	-0.0281	100	ASAS-SN
2458568.0307	2019-03-25	0.0006	g	16618	-0.0276	104	ASAS-SN
2458568.0307	2019-03-25	0.0006	g	16618	-0.0276	104	ASAS-SN
KZ Cen							
2412139.3277	1892-02-10	0.0349	PG	-15275	0.6057	18	DASCH
2414024.0446	1897-04-09	0.0176	PG	-14035	0.5483	20	DASCH
2415533.2679	1901-05-28	0.0148	PG	-13042	0.4323	37	DASCH
2416591.1134	1904-04-20	0.0116	PG	-12346	0.3722	61	DASCH
2417802.4834	1907-08-14	0.0144	PG	-11549	0.3187	37	DASCH
2418483.3956	1909-06-25	0.0266	PG	-11101	0.2803	24	DASCH
2419717.5425	1912-11-11	0.0288	PG	-10289	0.2040	14	DASCH
2420465.4008	1914-11-28	0.0090	PG	-9797	0.2325	33	DASCH
2420997.3634	1916-05-13	0.0224	PG	-9447	0.2023	21	DASCH
2421594.7083	1918-01-01	0.0121	PG	-9054	0.1954	34	DASCH
2422237.6385	1919-10-06	0.0107	PG	-8631	0.1744	44	DASCH
2423401.8983	1922-12-13	0.0193	PG	-7865	0.1301	28	DASCH
2424108.7184	1924-11-19	0.0256	PG	-7400	0.1599	49	DASCH
2424665.0129	1926-05-29	0.0277	PG	-7034	0.1419	20	DASCH
2425534.3823	1928-10-14	0.0110	PG	-6462	0.0833	57	DASCH
2426826.3695	1932-04-28	0.0104	PG	-5612	0.0880	33	DASCH
2427750.5052	1934-11-09	0.0138	PG	-5004	0.0764	55	DASCH
2428461.8158	1936-10-20	0.0122	PG	-4536	0.0367	52	DASCH
2429036.3619	1938-05-17	0.0121	PG	-4158	0.0306	46	DASCH
2429382.9298	1939-04-29	0.0100	PG	-3930	0.0433	55	DASCH
2429744.6756	1940-04-25	0.0098	PG	-3692	0.0341	47	DASCH
2430235.6173	1941-08-29	0.0078	PG	-3369	0.0225	112	DASCH
2430823.8547	1943-04-09	0.0148	PG	-2982	0.0279	41	DASCH
2431211.4461	1944-04-30	0.0092	PG	-2727	0.0246	79	DASCH
2431576.2239	1945-04-30	0.0114	PG	-2487	0.0074	60	DASCH
2431944.0651	1946-05-03	0.0124	PG	-2245	0.0136	69	DASCH
2432453.2514	1947-09-24	0.0081	PG	-1910	0.0069	133	DASCH
2433017.1442	1949-04-10	0.0124	PG	-1539	-0.0127	49	DASCH
2433617.5746	1950-12-02	0.0125	PG	-1144	0.0260	31	DASCH
2435228.7452	1955-05-01	0.0301	V	-84	0.0210	7	Irwin (1961)
2435228.7566	1955-05-01	0.0657	B	-84	0.0300	7	Irwin (1961)
2444059.8938	1979-07-05	0.0175	PG	5726	0.0877	42	DASCH
2445073.7337	1982-04-14	0.0005	V	6393	0.1040	171	Petersen & Hansen (1984)
2445073.7339	1982-04-14	0.0005	B	6393	0.1017	170	Petersen & Hansen (1984)

Table A1 – *Continued*

Max, HJD	Year	Uncertainty	Filter	E	O–C, days	N	Reference
2445969.0148	1984-09-25	0.0128	<i>PG</i>	6982	0.1148	43	DASCH
2446051.1029	1984-12-16	0.0018	<i>V</i>	7036	0.1265	9	Diethelm (1986)
2446051.1037	1984-12-16	0.0013	<i>B</i>	7036	0.1248	9	Diethelm (1986)
2446744.2247	1986-11-09	0.0129	<i>PG</i>	7492	0.1353	33	DASCH
2446871.9139	1987-03-17	0.0093	<i>PG</i>	7576	0.1462	77	DASCH
2451979.2030	2001-03-10	0.0045	<i>V</i>	10936	0.3075	80	ASAS-SN
2452543.1264	2002-09-25	0.0084	<i>V</i>	11307	0.3187	22	ASAS-SN
2452859.2930	2003-08-07	0.0026	<i>V</i>	11515	0.3296	159	ASAS-SN
2453485.5410	2005-04-25	0.0047	<i>V</i>	11927	0.3461	66	ASAS-SN
2453815.3988	2006-03-20	0.0052	<i>V</i>	12144	0.3684	68	ASAS-SN
2454218.2128	2007-04-27	0.0051	<i>V</i>	12409	0.3879	65	ASAS-SN
2454575.4186	2008-04-18	0.0038	<i>V</i>	12644	0.3986	82	ASAS-SN
2454926.5579	2009-04-05	0.0054	<i>V</i>	12875	0.4227	64	ASAS-SN
2456966.4488	2014-11-04	0.0009	<i>V</i>	14217	0.5015	180	ASAS-SN
2457167.0958	2015-05-24	0.0009	<i>V</i>	14349	0.5112	76	ASAS-SN
2457416.3860	2016-01-28	0.0009	<i>V</i>	14513	0.5249	140	ASAS-SN
2457557.7502	2016-06-18	0.0010	<i>V</i>	14606	0.5309	88	ASAS-SN
2457782.7184	2017-01-29	0.0009	<i>V</i>	14754	0.5422	140	ASAS-SN
2457908.8838	2017-06-04	0.0009	<i>V</i>	14837	0.5493	156	ASAS-SN
2458130.8059	2018-01-12	0.0008	<i>g</i>	14983	0.5545	100	ASAS-SN
2458177.9291	2018-02-28	0.0008	<i>g</i>	15014	0.5583	100	ASAS-SN
2458188.5724	2018-03-11	0.0009	<i>V</i>	15021	0.5617	202	ASAS-SN
2458222.0082	2018-04-13	0.0010	<i>g</i>	15043	0.5580	99	ASAS-SN
2458290.4128	2018-06-20	0.0007	<i>g</i>	15088	0.5635	172	ASAS-SN
2458480.4191	2018-12-27	0.0007	<i>g</i>	15213	0.5725	150	ASAS-SN
2458536.6604	2019-02-22	0.0006	<i>g</i>	15250	0.5745	150	ASAS-SN
2458576.1820	2019-04-02	0.0009	<i>g</i>	15276	0.5767	148	ASAS-SN
V745 Oph							
2413362.5270	1895-06-18	0.1197	<i>PG</i>	-14178	10.4186	4	DASCH
2413789.9750	1896-08-18	0.0139	<i>PG</i>	-13910	10.3788	6	DASCH
2414591.2173	1898-10-28	0.0148	<i>PG</i>	-13407	9.2839	7	DASCH
2415187.6688	1900-06-17	0.0113	<i>PG</i>	-13033	9.1665	4	DASCH
2415880.6617	1902-05-11	0.0529	<i>PG</i>	-12598	8.2893	5	DASCH
2416270.9350	1903-06-05	0.0110	<i>PG</i>	-12353	7.7621	7	DASCH
2417410.5773	1906-07-19	0.0184	<i>PG</i>	-11638	6.9052	5	DASCH
2418309.7250	1909-01-03	0.0082	<i>PG</i>	-11074	6.4143	5	DASCH
2420217.5768	1914-03-26	0.0085	<i>PG</i>	-9877	4.9269	7	DASCH
2421483.6332	1917-09-12	0.0190	<i>PG</i>	-9083	4.4709	5	DASCH
2423707.1064	1923-10-14	0.0103	<i>PG</i>	-7688	2.7742	10	DASCH
2424409.0761	1925-09-15	0.0210	<i>PG</i>	-7248	2.8983	7	DASCH
2424710.3520	1926-07-13	0.0144	<i>PG</i>	-7059	2.6996	10	DASCH
2425735.4703	1929-05-03	0.0147	<i>PG</i>	-6416	2.1661	8	DASCH
2427039.8129	1932-11-28	0.0115	<i>PG</i>	-5598	1.7138	7	DASCH
2427648.8494	1934-07-30	0.0060	<i>PG</i>	-5216	1.4206	38	DASCH
2427990.0895	1935-07-06	0.0058	<i>PG</i>	-5002	1.3085	28	DASCH
2428326.5944	1936-06-07	0.0066	<i>PG</i>	-4791	1.2465	30	DASCH
2428698.1951	1937-06-13	0.0073	<i>PG</i>	-4558	1.1880	17	DASCH
2429093.5450	1938-07-14	0.0067	<i>PG</i>	-4310	0.9522	23	DASCH
2429436.3147	1939-06-21	0.0117	<i>PG</i>	-4095	0.7745	16	DASCH
2429757.0430	1940-05-07	0.0098	<i>PG</i>	-3894	0.8870	12	DASCH
2429843.0930	1940-08-01	0.0102	<i>PG</i>	-3840	0.8014	15	DASCH
2430170.0167	1941-06-24	0.0091	<i>PG</i>	-3635	0.7288	19	DASCH
2430170.0167	1941-06-24	0.0091	<i>PG</i>	-3635	0.7288	19	DASCH
2430498.4792	1942-05-18	0.0129	<i>PG</i>	-3429	0.5999	9	DASCH
2430830.1848	1943-04-15	0.0067	<i>PG</i>	-3221	0.5240	8	DASCH
2431260.8527	1944-06-19	0.0078	<i>PG</i>	-2951	0.5138	16	DASCH
2431613.0968	1945-06-06	0.0095	<i>PG</i>	-2730	0.2400	13	DASCH
2431986.4350	1946-06-14	0.0076	<i>PG</i>	-2496	0.3239	20	DASCH

Table A1 – *Continued*

Max, HJD	Year	Uncertainty	Filter	E	O–C, days	N	Reference
2432351.6846	1947-06-15	0.0063	PG	-2267	0.2947	25	DASCH
2432699.3630	1948-05-27	0.0115	PG	-2049	0.2405	14	DASCH
2433072.6334	1949-06-05	0.0071	PG	-1815	0.2566	17	DASCH
2433463.2384	1950-06-30	0.0119	PG	-1570	0.0612	11	DASCH
2433814.1969	1951-06-16	0.0124	PG	-1350	0.0968	8	DASCH
2434085.2465	1952-03-13	0.0139	PG	-1180	-0.0212	8	DASCH
2434085.2465	1952-03-13	0.0139	PG	-1180	-0.0212	8	DASCH
2436910.2533	1959-12-07	0.0031	PGV	591	0.0801	7	Mandel (1970)
2437718.9536	1962-02-23	0.0050	PGV	1098	0.0628	8	Mandel (1970)
2437900.7784	1962-08-24	0.0030	VIS	1212	0.0458	19	Mandel (1970)
2438647.3305	1964-09-08	0.0034	PGV	1680	0.0893	14	Mandel (1970)
2440413.3918	1969-07-10	0.0106	PG	2787	0.3472	9	DASCH
2441287.6601	1971-12-02	0.0095	PG	3335	0.4986	9	DASCH
2441761.5661	1973-03-20	0.0045	V	3632	0.6823	40	Kwee & Diethelm (1984)
2441780.7308	1973-04-08	0.0060	B	3644	0.6823	37	Kwee & Diethelm (1984)
2442441.2786	1975-01-28	0.0143	PG	4058	0.8571	10	DASCH
2442934.2248	1976-06-04	0.0241	PG	4367	0.9163	8	DASCH
2443314.0155	1977-06-19	0.0143	PG	4605	1.0722	8	DASCH
2443314.0155	1977-06-19	0.0143	PG	4605	1.0722	8	DASCH
2443778.2868	1978-09-26	0.0090	PG	4896	1.1683	12	DASCH
2444569.7789	1980-11-26	0.0122	PG	5392	1.4890	8	DASCH
2444817.0688	1981-07-31	0.1301	PG	5547	1.5378	5	DASCH
2445279.8278	1982-11-06	0.0091	PG	5837	1.7166	18	DASCH
2445839.8933	1984-05-19	0.0096	PG	6188	1.9007	17	DASCH
2446232.5267	1985-06-16	0.0179	PG	6434	2.1386	13	DASCH
2446612.3828	1986-06-30	0.0133	PG	6672	2.3600	13	DASCH
2446987.3897	1987-07-10	0.0082	PG	6907	2.5174	8	DASCH
2447617.7538	1989-04-01	0.0122	PG	7302	2.8156	8	DASCH
2453876.0563	2006-05-20	0.0206	V	11223	6.7395	23	INTEGRAL-OMC
2454566.1551	2008-04-09	0.0159	V	11655	7.7534	18	INTEGRAL-OMC
2454645.3459	2008-06-27	0.0030	V	11705	7.1891	16	CSS
2454841.9214	2009-01-10	0.0164	V	11828	7.5667	13	CSS
2455101.8873	2009-09-27	0.0243	V	11991	7.5308	14	INTEGRAL-OMC
2456049.9321	2012-05-02	0.0384	V	12585	8.0838	16	CSS
2456115.5025	2012-07-07	0.0104	V	12626	8.2550	23	ASAS-SN
2456115.7236	2012-07-07	0.0068	V	12626	8.4761	24	CSS
2456342.3866	2013-02-18	0.0249	g	12768	8.6344	8	Chambers et al. (2016)
2456465.1982	2013-06-21	0.0029	V	12845	8.6230	70	ASAS-SN
2456790.8710	2014-05-13	0.0031	V	13049	8.8946	70	ASAS-SN
2456901.0270	2014-08-31	0.0029	V	13118	8.9885	67	ASAS-SN
2457110.1646	2015-03-28	0.0034	V	13249	9.1674	93	ASAS-SN
2457229.8946	2015-07-26	0.0024	V	13324	9.2646	95	ASAS-SN
2457461.3797	2016-03-13	0.0024	V	13469	9.4597	121	ASAS-SN
2457606.6689	2016-08-06	0.0027	V	13560	9.5945	125	ASAS-SN
2457844.5385	2017-04-01	0.0027	V	13709	9.7936	115	ASAS-SN
2457969.0712	2017-08-03	0.0035	V	13787	9.9082	126	ASAS-SN
2458184.6170	2018-03-07	0.0027	g	13922	10.1150	139	ASAS-SN
2458218.1310	2018-04-09	0.0046	V	13943	10.1318	67	ASAS-SN
2458282.0089	2018-06-12	0.0025	g	13983	10.2056	135	ASAS-SN
2458304.3379	2018-07-04	0.0034	V	13997	10.2031	71	ASAS-SN
2458379.3699	2018-09-17	0.0041	V	14044	10.2652	22	ASAS-SN
2458419.3105	2018-10-27	0.0044	g	14069	10.3282	62	ASAS-SN
2458567.7945	2019-03-25	0.0034	g	14162	10.4676	58	ASAS-SN
V439 Oph							
2413120.8627	1894-10-19	0.0087	PG	-11615	0.2469	13	DASCH
2415417.0420	1901-02-01	0.0061	PG	-10402	0.2257	29	DASCH
2416798.8860	1904-11-14	0.0048	PG	-9672	0.1850	40	DASCH
2422273.3222	1919-11-10	0.0063	PG	-6780	0.0855	140	DASCH

Table A1 – *Continued*

Max, HJD	Year	Uncertainty	Filter	E	O–C, days	N	Reference
2426172.8662	1930-07-15	0.0060	<i>PG</i>	-4720	0.0640	42	DASCH
2426574.1821	1931-08-20	0.0082	<i>VIS</i>	-4508	0.0559	50	Tsesevich (1952)
2427543.3797	1934-04-15	0.0062	<i>PG</i>	-3996	0.0506	88	DASCH
2428151.0264	1935-12-14	0.0058	<i>PG</i>	-3675	0.0466	111	DASCH
2428944.1601	1938-02-14	0.0080	<i>PG</i>	-3256	0.0163	84	DASCH
2429814.9538	1940-07-04	0.0057	<i>PG</i>	-2796	0.0332	119	DASCH
2430337.4285	1941-12-08	0.0088	<i>PG</i>	-2520	0.0419	17	SAI (this paper)
2431105.9344	1944-01-16	0.0057	<i>PG</i>	-2114	-0.0074	157	DASCH
2432177.3898	1946-12-22	0.0087	<i>PG</i>	-1548	0.0140	78	DASCH
2432894.8408	1948-12-09	0.0065	<i>PG</i>	-1169	0.0207	94	DASCH
2433739.1133	1951-04-02	0.0078	<i>PG</i>	-723	0.0183	86	DASCH
2437439.8443	1961-05-20	0.0052	<i>PGV</i>	1232	-0.0614	122	Mandel (1970)
2438810.4112	1965-02-18	0.0057	<i>B</i>	1956	-0.0119	21	Sturch (1966)
2438818.0126	1965-02-26	0.0035	<i>V</i>	1960	0.0081	22	Sturch (1966)
2442056.9553	1974-01-09	0.0051	<i>PG</i>	3671	0.0493	46	DASCH
2443673.5826	1978-06-14	0.0062	<i>B</i>	4525	0.0607	22	Henden (1980)
2443675.4881	1978-06-15	0.0027	<i>V</i>	4526	0.0636	20	Henden (1980)
2443775.7689	1978-09-24	0.0045	<i>PG</i>	4579	0.0254	98	SAI (this paper)
2444065.4552	1979-07-10	0.0114	<i>V</i>	4732	0.0742	6	Diethelm & Tamman (1982)
2444067.3706	1979-07-12	0.0204	<i>B</i>	4733	0.1061	8	Diethelm & Tamman (1982)
2446058.7600	1984-12-24	0.0076	<i>PG</i>	5785	0.0669	120	DASCH
2457083.7467	2015-03-02	0.0026	<i>V</i>	11609	0.2532	162	ASAS-SN
2457468.0424	2016-03-20	0.0033	<i>V</i>	11812	0.2714	90	ASAS-SN
2457602.4414	2016-08-01	0.0034	<i>V</i>	11883	0.2679	93	ASAS-SN
2457914.7930	2017-06-10	0.0022	<i>V</i>	12048	0.2756	181	ASAS-SN
2458223.3601	2018-04-14	0.0044	<i>V</i>	12211	0.2848	90	ASAS-SN
2458276.3162	2018-06-06	0.0012	<i>g</i>	12239	0.2371	90	ASAS-SN
2458327.4767	2018-07-27	0.0032	<i>V</i>	12266	0.2868	103	ASAS-SN
2458367.1816	2018-09-05	0.0022	<i>g</i>	12287	0.2389	84	ASAS-SN
2458564.0546	2019-03-21	0.0015	<i>g</i>	12391	0.2406	118	ASAS-SN

This paper has been typeset from a $\text{\TeX}/\text{\LaTeX}$ file prepared by the author.